Available online at www.sciencedirect.com
SCIENCE DIRECT
Physics Letters B 634 (2006) 148–154
PHYSICS LETTERS B
www.elsevier.com/locate/physletb

Study of the decay $\phi \to f_0(980)\gamma \to \pi^+\pi^-\gamma$ with the KLOE detector

KLOE Collaboration

F. Ambrosino [f], A. Antonelli [b], M. Antonelli [b], C. Bacci [k], P. Beltrame [c], G. Bencivenni [b], S. Bertolucci [b], C. Bini [i,*], C. Bloise [b], V. Bocci [i], F. Bossi [b], D. Bowring [b,m], P. Branchini [k], R. Caloi [i], P. Campana [b], G. Capon [b], T. Capussela [f], F. Ceradini [k], S. Chi [b], G. Chiefari [f], P. Ciambrone [b], S. Conetti [m], E. De Lucia [b], A. De Santis [i], P. De Simone [b], G. De Zorzi [i], S. Dell'Agnello [b], A. Denig [c], A. Di Domenico [i], C. Di Donato [f], S. Di Falco [g], B. Di Micco [k], A. Doria [f], M. Dreucci [b], G. Felici [b], A. Ferrari [b], M.L. Ferrer [b], G. Finocchiaro [b], S. Fiore [i], C. Forti [b], P. Franzini [i], C. Gatti [b], P. Gauzzi [i], S. Giovannella [b], E. Gorini [d], E. Graziani [k], M. Incagli [g], W. Kluge [c], V. Kulikov [e], F. Lacava [i], G. Lanfranchi [b], J. Lee-Franzini [b,l], D. Leone [c], M. Martini [b], P. Massarotti [f], W. Mei [b], S. Meola [f], S. Miscetti [b], M. Moulson [b], S. Müller [c], F. Murtas [b], M. Napolitano [f], F. Nguyen [k], M. Palutan [b], E. Pasqualucci [i], A. Passeri [k], V. Patera [b,h], F. Perfetto [f], L. Pontecorvo [i], M. Primavera [d], P. Santangelo [b], E. Santovetti [j], G. Saracino [f], B. Sciascia [b], A. Sciubba [b,h], F. Scuri [g], I. Sfiligoi [b], T. Spadaro [b], M. Testa [i], L. Tortora [k], P. Valente [i], B. Valeriani [c], G. Venanzoni [b], S. Veneziano [i], A. Ventura [d], S. Ventura [i], R. Versaci [c], G. Xu [a,b]

[a] *Institute of High Energy Physics of Academica Sinica, Beijing, China*
[b] *Laboratori Nazionali di Frascati dell'INFN, Frascati, Italy*
[c] *Institut für Experimentelle Kernphysik, Universität Karlsruhe, Germany*
[d] *Dipartimento di Fisica dell'Università e Sezione INFN, Lecce, Italy*
[e] *Institute for Theoretical and Experimental Physics, Moscow, Russia*
[f] *Dipartimento di Scienze Fisiche dell'Università "Federico II" e Sezione INFN, Napoli, Italy*
[g] *Dipartimento di Fisica dell'Università e Sezione INFN, Pisa, Italy*
[h] *Dipartimento di Energetica dell'Università "La Sapienza", Roma, Italy*
[i] *Dipartimento di Fisica dell'Università "La Sapienza" e Sezione INFN, Roma, Italy*
[j] *Dipartimento di Fisica dell'Università "Tor Vergata" e Sezione INFN, Roma, Italy*
[k] *Dipartimento di Fisica dell'Università "Roma Tre" e Sezione INFN, Roma, Italy*
[l] *Physics Department, State University of New York at Stony Brook, USA*
[m] *Physics Department, University of Virginia, USA*

Received 11 November 2005; received in revised form 19 December 2005; accepted 13 January 2006

Available online 2 February 2006

Editor: L. Rolandi

Abstract

We measured, with the KLOE detector, the spectrum of $\pi^+\pi^-$ invariant mass in a sample of 6.7×10^5 $e^+e^- \to \pi^+\pi^-\gamma$ events with the photon at large polar angle ($\theta_\gamma > 45°$) at a centre of mass energy $\sqrt{s}$ around the ϕ mass. We observe in this spectrum a clear contribution from the intermediate process $\phi \to f_0(980)\gamma$. A sizeable effect is also observed in the distribution of the pion forward–backward asymmetry. We use different theoretical models to fit the spectrum and we determine the f_0 mass and coupling constants to the ϕ, to $\pi^+\pi^-$ and to $K\bar{K}$.

* Corresponding author. Tel.: +390649914266; fax: +39064957697.
E-mail address: cesare.bini@roma1.infn.it (C. Bini).

0370-2693/$ – see front matter © 2006 Elsevier B.V. All rights reserved.
doi:10.1016/j.physletb.2006.01.016

PACS: 13.20.-v; 13.20.Jf

Keywords: Radiative decays of mesons; Decays of other mesons

1. Introduction

The $\phi(1020)$ radiative decays to $f_0(980)$ and $a_0(980)$ play an important role in the investigation of the controversial structure of the lighter scalar mesons [1,2]. At KLOE, we detect the f_0 through its decay to $\pi\pi$ via the decay chain $e^+e^- \to \phi \to f_0 \to \pi\pi\gamma$. KLOE has already published studies on ϕ decays to $f_0\gamma$ and $a_0\gamma$ looking for the final states $\pi^0\pi^0\gamma$ [3] and $\eta\pi^0\gamma$ [4], respectively. On the contrary, the decay chain $e^+e^- \to \phi \to f_0(a_0) \to K\bar{K}\gamma$ is kinematically suppressed, and has not been observed yet. In this Letter we present a study of the f_0 decay to $\pi^+\pi^-$, based on an integrated luminosity of 350 pb^{-1} collected at the collider DAΦNE during the years 2001 and 2002, at a centre of mass energy $\sqrt{s}$ around the ϕ mass $m_\phi = 1019.45$ MeV within ± 0.5 MeV ("on-peak" data). The only previous search for this decay has been published by the CMD-2 Collaboration [5], mainly based on an energy scan around the ϕ mass peak.

We look for $f_0 \to \pi^+\pi^-$ decays in events $e^+e^- \to \pi^+\pi^-\gamma$. Only a small fraction of the $\pi^+\pi^-\gamma$ events originates from the radiative decay $\phi \to f_0\gamma$ with $f_0 \to \pi^+\pi^-$. The main contribution is given by $e^+e^- \to \pi^+\pi^-\gamma$ events with a photon from initial state (ISR) or final state (FSR) radiation. The amplitude of each contribution is characterised by a different spectrum of the $\pi^+\pi^-$ invariant mass m, and of the photon polar angle θ_γ measured with respect to the beam axis. In particular, the ISR is the dominant contribution for small photon polar angles, allowing to extract the $e^+e^- \to \pi^+\pi^-$ cross-section below the ϕ mass with the so-called radiative return method [6]; at large values of θ_γ the ISR contribution is strongly reduced, so that the other processes can be observed in this region only. A smaller contribution comes from the decay $\phi \to \rho^\pm\pi^\mp$ with $\rho^\pm \to \pi^\pm\gamma$ (we call it $\rho\pi$ term in the following). It contributes in the low mass region, $400 < m < 600$ MeV, with total branching ratio $\mathrm{BR}(\phi \to \rho^\pm\pi^\mp) \times \mathrm{BR}(\rho^\pm \to \pi^\pm\gamma) \sim 4 \times 10^{-5}$. Finally, the possibility to observe the decay chain $\phi \to f_0(600)\gamma \to \pi^+\pi^-\gamma$ is considered.

The $\pi^+\pi^-$ pair has different quantum numbers whether it is produced through FSR and f_0 decay or ISR: $J^{PC} = 0^{++}$ in the former case, and $J^{PC} = 1^{--}$ in the latter. A sizeable interference term between FSR and f_0 decay is expected in the m spectrum. On the other hand, any interference term between two amplitudes of opposite charge conjugation gives rise to C-odd terms that change sign by the interchange of the two pions. Therefore, the interference between ISR and FSR or f_0 decay, results in a null contribution in the m spectrum for symmetric cuts on θ_γ and $\theta_{\pi^\pm}$, and in a sizable forward–backward asymmetry, A_c, defined as:

$$A_c = \frac{N(\theta_{\pi^+} > 90°) - N(\theta_{\pi^+} < 90°)}{N(\theta_{\pi^+} > 90°) + N(\theta_{\pi^+} < 90°)}, \qquad (1)$$

where the angle θ_{π^+} is defined with respect to the direction of the incoming electron beam.

2. Experimental set-up

DAΦNE is an e^+e^--collider with a peak luminosity of about 10^{32} $cm^{-2}\,s^{-1}$ at a centre of mass energy $\sqrt{s} = m_\phi = 1.02$ GeV. The beams collide with a crossing angle of $\pi - 0.025$ rad. The KLOE detector consists of a large-volume cylindrical drift chamber [7] (3.3 m length and 2 m radius), operated with a 90% helium–10% isobutane gas mixture, surrounded by a sampling calorimeter [8] made of lead and scintillating fibres providing a solid angle coverage of 98%. The tracking chamber and the calorimeter are surrounded by a superconducting coil that produces a solenoidal field $B = 0.52$ T. The drift chamber has a momentum resolution of $\sigma(p_\perp)/p_\perp \sim 0.4\%$. Photon energies and arrival times are measured by the calorimeter with resolutions of $\sigma_E/E = 5.7\%/\sqrt{E(\mathrm{GeV})}$ and $\sigma_t = 54\ \mathrm{ps}/\sqrt{E(\mathrm{GeV})} \oplus 50$ ps. The trigger [9] is based on the detection of at least two energy deposits in the calorimeter above a threshold that ranges between 50 and 150 MeV. The trigger includes a cosmic ray veto based on large energy deposits in the outermost calorimeter layers.

3. Event selection

We select $\pi^+\pi^-\gamma$ events by requiring a reconstructed vertex close to the interaction region with two tracks of opposite charge, emitted with polar angles above 45° ($\theta_{\pi^\pm} > 45°$). We suppress the ISR component by requiring the polar angle of the total missing momentum to be larger than 45° ($\theta_\gamma > 45°$). Both tracks are extrapolated to the calorimeter. A likelihood variable, based on the time of flight and on the shower profile (see Ref. [6]), is used to select pions. A cut on this variable reduces the background due to $e^+e^-\gamma$ events to a negligible level.

In order to remove $\pi^+\pi^-\pi^0$ and $\mu^+\mu^-\gamma$ events, we define the track mass variable M_T as the solution of the equation:

$$|\vec{p}_\phi - \vec{p}_1 - \vec{p}_2| = E_\phi - \sqrt{p_1^2 + M_T^2} - \sqrt{p_2^2 + M_T^2}, \qquad (2)$$

where $\vec{p}_1$ and $\vec{p}_2$ are the momenta of the two tracks, and where E_ϕ and $\vec{p}_\phi$ are the ϕ energy and momentum, respectively. These are evaluated run by run using samples of Bhabha scattering events. Eq. (2) is verified by events with two particles of mass M_T and a third particle with null mass. M_T is required to be equal to the pion mass within ± 10 MeV. To reduce the residual $\pi^+\pi^-\pi^0$ contamination and to remove badly reconstructed $e^+e^- \to \pi^+\pi^-$ events with soft photon emitted, we require a calorimeter cluster matching the missing energy and momentum. The cluster is required to be non-associated to tracks, to have an energy $E_\gamma > 10$ MeV, and to have a time compatible with a photon coming from the interaction vertex,

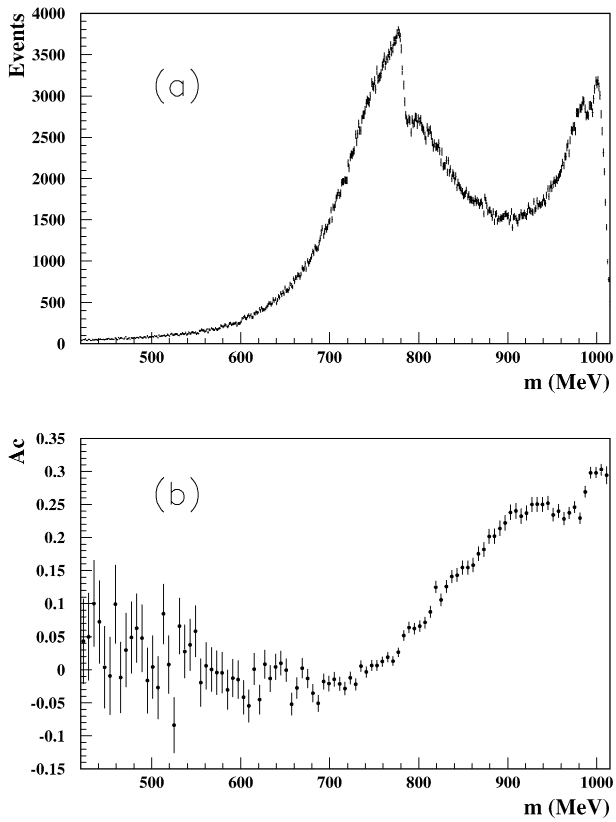

Fig. 1. (a) $\pi^+\pi^-$ invariant mass spectrum of the selected sample. The spectrum is dominated by the ISR component, showing the ρ–ω interference pattern. The signal of the $f_0(980)$ appears as a small peak around 980 MeV. The drop for $m > 1000$ MeV is due to the drop of the detection efficiency for low energy photons. (b) Forward–backward asymmetry defined in Eq. (1) as a function of m. The dip in the region of the $f_0(980)$ is evident.

$|t_\gamma - R_\gamma/c| < 5\sigma_t(E_\gamma)$, where t_γ is the cluster time, R_γ is the flight distance, and $\sigma_t(E_\gamma)$ is the time resolution for photons of energy E_γ. The requirement $E_\gamma > 10$ MeV translates in an effective cut $m < 1009$ MeV. Finally, the angle Ω between the missing momentum and the photon direction derived from the cluster position, has to be below $0.03 + 3/E_\gamma(\text{MeV})$ rad. The dependence of the Ω cut on E_γ reflects that of the cluster position resolution on the photon energy.

We select 6.7×10^5 events. The spectrum of the $\pi\pi$ invariant mass m for these events and the forward–backward asymmetry dependence on m are shown in Fig. 1. We observe a small bump in the m spectrum in the region where the $f_0(980)$ is expected to be. A signal is observed also as a dip in the forward–backward asymmetry A_c, for the same values of m.

Total efficiency and residual background distributions are shown in Fig. 2, as evaluated by Monte Carlo with corrections based on data control samples [10]. The simulation of the ISR and FSR contributions is based on the EVA generator [11]. The efficiency decrease at low masses is due to the increased occurrence of low-p_T pions with $\theta_{\pi^\pm} < 45°$ that escape the selection; the decrease for higher masses, starting from ~ 800 MeV, is partly due to the cosmic ray veto and partly to the photon detection efficiency. In fact, high momentum pions, which deposit large energy in the outermost calorimeter layers, veto the event with high probability. Moreover, low energy photons ($E_\gamma < 20$ MeV) are detected with an efficiency lower than 80%. The efficiency for the cosmic veto is evaluated using samples of pre-scaled events with no veto applied. The photon detection efficiency is measured as a function of E_γ from $\pi^+\pi^-\pi^0$ and $e^+e^-\gamma$ control samples [8].

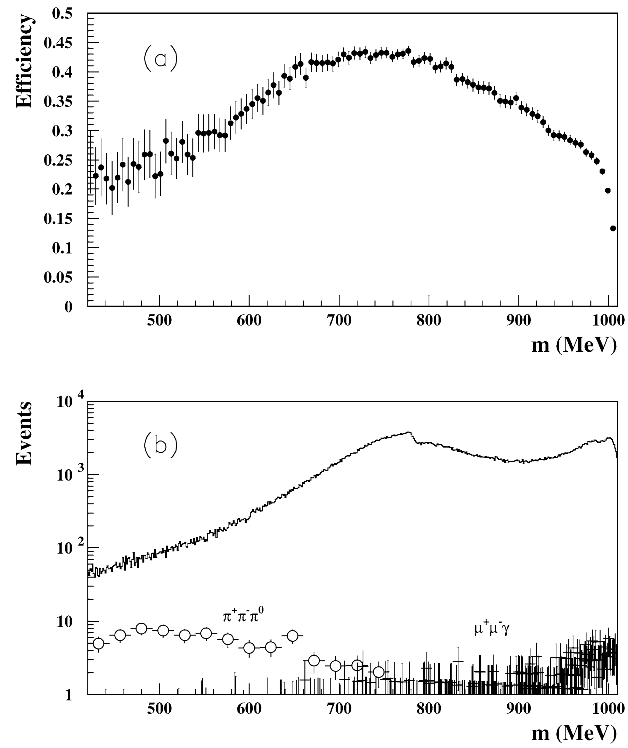

Fig. 2. (a) Total efficiency as a function of m. (b) The Monte Carlo expected contributions of the main background sources, $\pi^+\pi^-\pi^0$ (open circles) and $\mu^+\mu^-\gamma$ (crosses), normalised to the integrated luminosity, and compared to the data spectrum.

After the selection, $\phi \to \pi^+\pi^-\pi^0$ decays give the only significant contribution to the background.

4. Description of the fit

We fit the $\pi^+\pi^-$ invariant mass spectrum, dN/dm, with the function:

$$\frac{dN}{dm} = L_{\text{int}}\epsilon(m)\left(\frac{d\sigma_{\text{ISR}}}{dm} + \frac{d\sigma_{\text{FSR}}}{dm} + \frac{d\sigma_{\rho\pi}}{dm} + \frac{d\sigma_{\text{scal}}}{dm} \pm \frac{d\sigma^{\text{INT}}_{\text{scal+FSR}}}{dm}\right) + \text{back}, \quad (3)$$

where L_{int} is the integrated luminosity, $\epsilon(m)$ is the selection efficiency, and *back* is the residual background. The first three terms in parenthesis are here called the "non-scalar" terms. The analytic expressions for the first and second terms, ISR and FSR, are taken from Ref. [12], while the $\rho\pi$ term is taken from Ref. [13]. The pion form factor [14], entering the ISR term, depends on the masses and widths of the ρ^0, ω and ρ' mesons, and on the two non-dimensional parameters α and β, which correspond to the sizes of the ω and ρ' contributions, respectively. We leave the quantities m_{ρ^0}, Γ_{ρ^0}, α, and β as free parameters of the fit while the masses and the widths of the ω and ρ' mesons are fixed to the PDG values [15]. The $\rho\pi$ term is multiplied by a scale factor, $a_{\rho\pi}$, which is expected to be equal to unity. If $a_{\rho\pi}=1$ the number of $\rho\pi$ events corresponds to approximately 1% of the total, broadly distributed in the low mass region. The possible interference between the $\rho\pi$ and the scalar terms is neglected. The last two terms in parenthesis, scal and scal + FSR, depend on the amplitude for the decay $\phi \to f_0\gamma \to \pi^+\pi^-\gamma$, the latter being the interference term between f_0 and FSR. The scal + FSR term can be either added (constructive interference) or subtracted (destructive interference).

We perform three fits corresponding to three different approaches in the description of the scalar amplitude.

The first fit is the kaon–loop fit (KL) [1,12]: the ϕ couples to the scalar through a loop of charged kaons. The formalism allows the inclusion of more than one scalar meson. For each scalar meson there are three free parameters of the fit: the mass and the couplings to K^+K^- and to $\pi^+\pi^-$. For the f_0 scalar meson only, the amplitude reduces to:

$$A_{\mathrm{KL}} = g\big(m^2\big)e^{i\delta(m)}\frac{g_{f_0K^+K^-}g_{f_0\pi^+\pi^-}}{(s-m^2)D'_{f_0}(m)}, \tag{4}$$

where s is the square of the centre of mass energy, $g_{f_0K^+K^-}$ and $g_{f_0\pi^+\pi^-}$ are the two couplings, $g(m^2)$ is the kaon–loop function [1], $\delta(m)$ is the phase of the background to the $\pi\pi$ elastic scattering, and D'_{f_0} is the f_0 inverse propagator with the finite width corrections [1].

In the second fit, called no-structure fit (NS) [16], a direct coupling $g_{\phi f_0\gamma}$ of the ϕ to the f_0 is assumed, with a subsequent coupling $g_{f_0\pi^+\pi^-}$ of the f_0 to the $\pi^+\pi^-$ pair. The f_0 amplitude is a Breit–Wigner with a mass dependent width [17] added to a polynomial complex function, the continuum, to allow an appropriate dumping of the resulting line shape. The amplitude depends on eight parameters: the mass m_{f_0}; the three couplings $g_{\phi f_0\gamma}$, $g_{f_0\pi^+\pi^-}$, and $g_{f_0K^+K^-}$; four parameters describing the continuum: two coefficients a_0 and a_1 and two phases b_0 and b_1. The amplitude is:

$$A_{\mathrm{NS}} = \frac{g_{\phi f_0\gamma}\,g_{f_0\pi^+\pi^-}}{D_{f_0}(m)} + \frac{a_0}{m_\phi^2}e^{ib_0p_\pi(m)} + a_1\frac{m^2-m_{f_0}^2}{m_\phi^4}e^{ib_1p_\pi(m)}, \tag{5}$$

where $p_\pi(m)=\sqrt{m^2/4-m_\pi^2}$ is the π momentum in the f_0 rest frame and $D_{f_0}(m)$ is the f_0 inverse propagator:

$$D_{f_0}(m) = m^2 - m_{f_0}^2 + i\left(\frac{g_{f_0\pi\pi}^2}{16\pi}\sqrt{1-\frac{4m_\pi^2}{m^2}} + \frac{g_{f_0KK}^2}{16\pi}\left(\sqrt{1-\frac{4m_{K^\pm}^2}{m^2}} + \sqrt{1-\frac{4m_{K^0}^2}{m^2}}\right)\right), \tag{6}$$

where $g_{f_0\pi\pi}=\sqrt{3/2}\,g_{f_0\pi^+\pi^-}$ and $g_{f_0KK}=g_{f_0K^+K^-}=g_{f_0K^0\overline{K^0}}$. These couplings have the same meaning as those defined within the KL frame and are related to the non-dimensional couplings g_π and g_K (see for instance [18,19]) through the relations $g_\pi \sim g_{f_0\pi\pi}^2/(8\pi m_{f_0}^2)$ and $g_K \sim g_{f_0KK}^2/(4\pi m_{f_0}^2)$ strictly valid only when $m\sim m_{f_0}$. In order to obtain the correct phase behaviour consistently with chiral perturbation theory predictions [20], b_0 is expressed as a function of the other parameters, reducing the free parameters to seven.

Finally in the scattering amplitudes (SA) fit [21] the amplitude is the sum of the scattering amplitudes $T_{11}=T(\pi\pi\to\pi\pi)$ and $T_{12}=T(\pi\pi\to KK)$, whose shapes are fixed by independent experimental information [22]:

$$A_{\mathrm{SA}} = \big(m-m_0^2\big)\left(1-\frac{m^2}{s}\right)\big[\big(a_1+b_1m^2+c_1m^4\big)T_{11} + \big(a_2+b_2m^2+c_2m^4\big)T_{12}\big]e^{i\lambda}, \tag{7}$$

free parameters are the six coefficients of the two polynomials, m_0 and the phase λ. Once the amplitude is determined by the fit, it is analytically continued in the complex m plane and the coupling g_ϕ is determined by the pole residue. The coupling g_ϕ, having the dimension of an energy, is connected to the partial width $\Gamma(\phi\to\gamma f_0(980))$ through the relation [21]:

$$\Gamma\big(\phi\to\gamma f_0(980)\big) = \frac{\pi^2}{2}g_\phi^2\frac{m_\phi^2-m_{f_0}^2}{m_\phi^3}. \tag{8}$$

5. Results

We fit the data in the region $420 < m < 1010$ MeV, using bins 1.2 MeV wide [23].

First we discuss the fits KL and NS. In both cases, a destructive interference is preferred by the fit for the $(d\sigma/dm)^{\mathrm{INT}}_{\mathrm{scal+FSR}}$ term, while the constructive interference is strongly disfavoured. The results are shown in Fig. 3, the χ^2 of the fits and the values of the parameters are given in Table 1. The non-scalar part is well described by the parametrisation used, while we are clearly not sensitive to the $\rho\pi$ term. The f_0 signal appears as an excess of events in the region between 900 and 1000 MeV. In the KL fit, the attempt to include a second scalar meson (the $f_0(600)$ or σ), with either E791 [24] or BES [25] masses (respectively 478 and 541 MeV), and with free couplings, gives no improvement to the fit. Moreover, since the couplings preferred by the fit are compatible with zero, within the statistical errors, the $f_0(600)$ is unnecessary to describe these data.

After the subtraction of the non-scalar part obtained in the KL and NS fits, an asymmetric peak around 980 MeV with a FWHM of 30–35 MeV and a height $\sim 25\%$ of the total is obtained, as shown in Fig. 3(c) and (f). Such a peak does not directly represent the f_0 shape but it results from the sum of a broad term $(d\sigma/dm)_{\mathrm{scal}}$ and a negative interference term $(d\sigma/dm)_{\mathrm{scal+FSR}}$ that cancels the low mass tail. The NS fit requires a significantly larger value of β than the KL fit does. This results in a non-scalar part $\sim 4\%$ larger in the f_0 peak region, and hence a correspondingly smaller signal size.

In order to assign the uncertainty to the parameters extracted from the fits, we have done a study of several systematic effects [23]. We have repeated the fits by varying the following quantities: the luminosity value around its total estimated error ($\sim 1\%$ [26]); the shape of the photon efficiency and the linearity of the

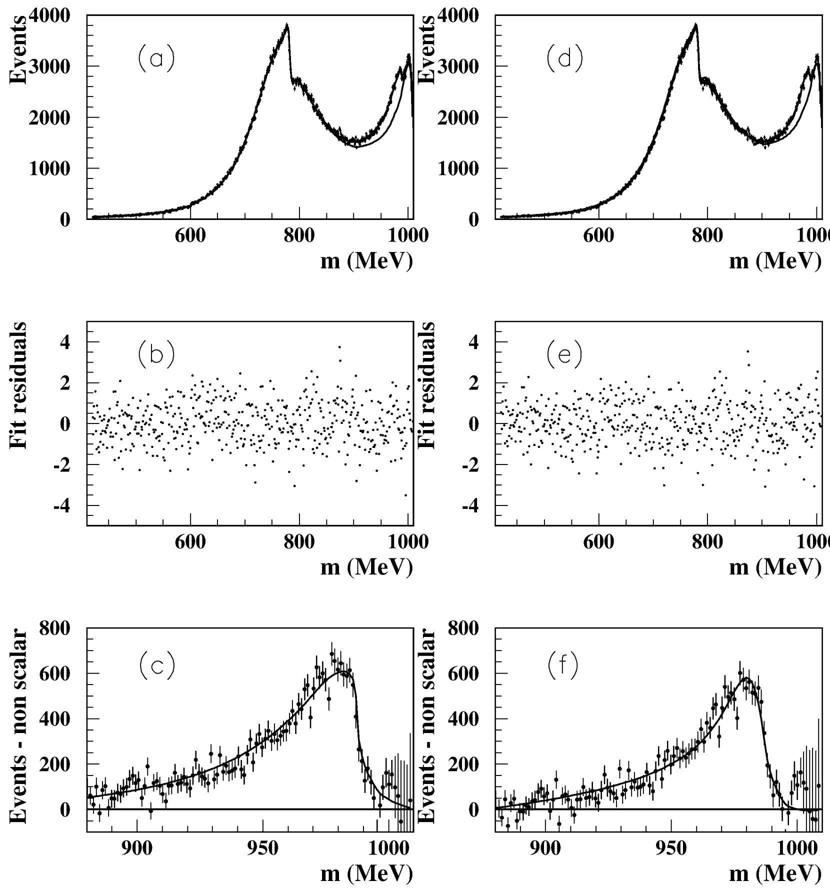

Fig. 3. Result of the KL fit (a)–(b)–(c) and of the NS fit (d)–(e)–(f). (a)–(d) Data spectrum compared with the fitting function (upper curve following the data points) and with the estimated non-scalar part of the function (lower curve); (b)–(e) fit residuals as a function of m; (c)–(f) the fitting function is compared to the spectrum obtained subtracting to the measured data the non-scalar part of the function in the f_0 region.

Table 1
Parameter results and χ^2 of the two fits KL (kaon–loop) and NS (no-structure). The results given in parentheses are not directly parameters of the fits but are evaluated as functions of the fit parameters

	KL	NS
χ^2 ($p(\chi^2)$)	538/483 (4.2%)	533/479 (4.4%)
m_{f_0} (MeV)	983.0 ± 0.6	977.3 ± 0.9
$g_{\phi f_0 \gamma}$ (GeV^{-1})	–	1.48 ± 0.06
$g_{f_0 K^+K^-}$ (GeV)	5.89 ± 0.14	1.73 ± 0.12
$g_{f_0 \pi^+\pi^-}$ (GeV)	(3.6)	0.99 ± 0.02
$R = g^2_{f_0 K^+K^-}/g^2_{f_0 \pi^+\pi^-}$	2.66 ± 0.10	(3.1)
a_0	–	6.00 ± 0.02
a_1	–	4.10 ± 0.04
b_1 (rad/GeV)	–	3.13 ± 0.05
m_{ρ^0} (MeV)	773.1 ± 0.2	773.0 ± 0.1
Γ_{ρ^0} (MeV)	144.0 ± 0.3	145.1 ± 0.1
α ($\times 10^{-3}$)	1.65 ± 0.05	1.64 ± 0.04
β ($\times 10^{-3}$)	-123 ± 1	-137 ± 1
$a_{\rho\pi}$	0.0 ± 0.6	1.5 ± 1.4

Table 2
Intervals of maximal variations for the f_0 parameters resulting from the systematic uncertainties studies done on both fits. Notice that the intervals obtained are larger than the fit uncertainties given in the previous table

Parameter	KL	NS
m_{f_0} (MeV)	980–987	973–981
$g_{f_0 K^+K^-}$ (GeV)	5.0–6.3	1.6–2.3
$g_{f_0 \pi^+\pi^-}$ (GeV)	3.0–4.2	0.9–1.1
$R = g^2_{f_0 K^+K^-}/g^2_{f_0 \pi^+\pi^-}$	2.2–2.8	2.6–4.4
$g_{\phi f_0 \gamma}$ (GeV^{-1})	–	1.2–2.0

photon response curves; the size of the $\pi^+\pi^-\pi^0$ background; the bin size, and the start and end points of the fit. While repeating the fits, the parameters of the non-scalar part are held fixed to their baseline values. Finally in order to take into account the systematic effect due to the limited knowledge of the non-scalar part of the spectrum, the NS fit has been repeated using the non-scalar parameters obtained from the KL fit and vice versa. In Table 2 we give the maximal variation intervals for the parameters, resulting from the studies discussed above.

The two fits have slightly overlapping intervals for the f_0 mass, and are both in agreement with the PDG interval 980 ± 10 MeV. We observe a large discrepancy between the KL and NS couplings $g_{f_0\pi^+\pi^-}$ and $g_{f_0 K^+K^-}$. The KL fit gives couplings in reasonable agreement with the KLOE results obtained with the final state $\pi^0\pi^0\gamma$ [3]. The two fits are in agreement on the ratio $R = g^2_{f_0 K^+K^-}/g^2_{f_0\pi^+\pi^-}$, pointing to an f_0 more coupled to kaons than to pions. Finally if we define an effective branching ratio as the integral over the full spec-

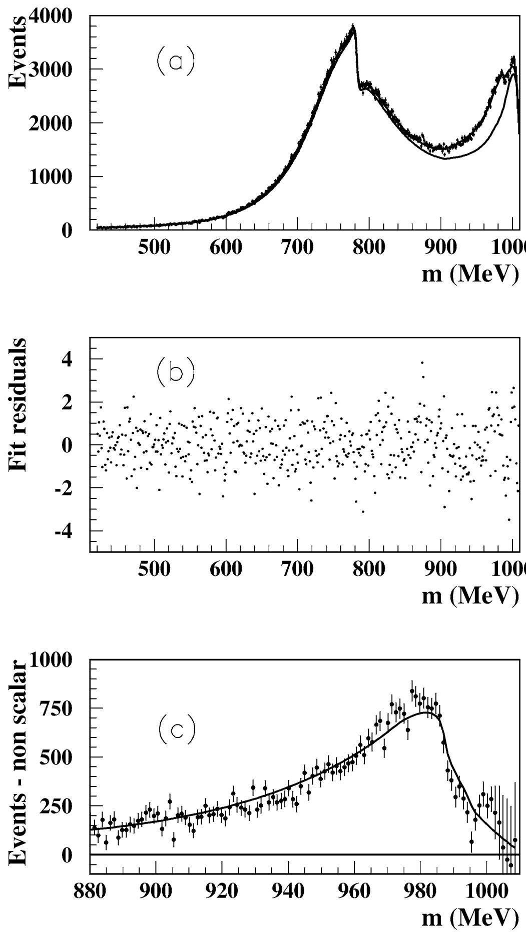

Fig. 4. Same as Fig. 3 for fit SA. In this case the fit lowers the non-scalar part and gives a larger signal than in the KL and NS fits. In the peak region the fit is clearly poorer than KL and NS fits.

Table 3
Results of SA fit. The χ^2 and the numerical values of the parameters are given together with the resulting values for the parameters of the non-scalar part

χ^2 ($p(\chi^2)$)	577/477 (0.1%)				
a_1	11.9	a_2	-14.7	m_{ρ^0} (MeV)	774.4 ± 0.2
b_1	3.3	b_2	-15.3	Γ_{ρ^0} (MeV)	142.8 ± 0.3
c_1	-15.1	c_2	35.8	α ($\times 10^{-3}$)	1.74 ± 0.05
m_0	0.	λ	-1.63	β ($\times 10^{-3}$)	-100 ± 18
				$a_{\rho\pi}$	0 ± 2

trum of the f_0 term normalised to the total ϕ width, we obtain $\mathrm{BR}(\phi \to f_0(980)\gamma) \times \mathrm{BR}(f_0(980) \to \pi^+\pi^-) = 2.1 \times 10^{-4}$ and 2.4×10^{-4} for KL and NS fits, respectively.

The SA fit is shown in Fig. 4 and in Table 3. The χ^2 is poorer especially in the f_0 peak region. Notice that a much better χ^2 can be hardly expected since T_{11} and T_{12} are derived from data sets that are less accurate than the data presented here. In any case by properly normalising the amplitude we obtain a value $g_\phi \sim 6.6 \times 10^{-4}$ GeV, in agreement with the value obtained in Ref. [21] by fitting the KLOE data on $\pi^0\pi^0\gamma$ together with other data. However we stress that such a value corresponds to an effective branching ratio of $\sim 3 \times 10^{-5}$, one order of magnitude lower than the one obtained from the other two fits. This

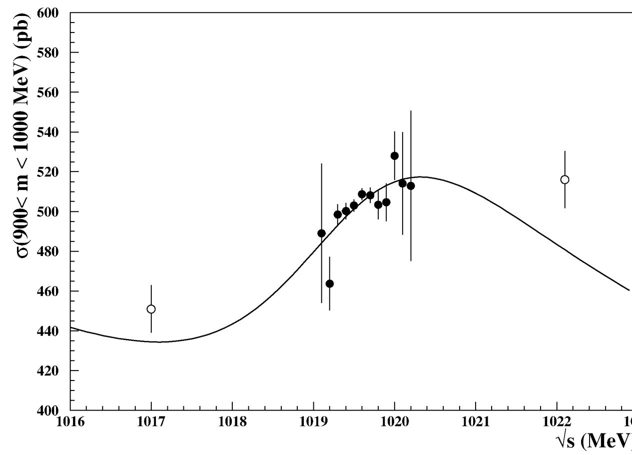

Fig. 5. Centre of mass energy dependence of the cross-section for events with m in the range 900–1000 MeV. The open points are the "on-peak" data sliced in 0.1 MeV wide bins, the full points are the "off-peak" data. The curve is the absolute prediction based on the KL fit parameters.

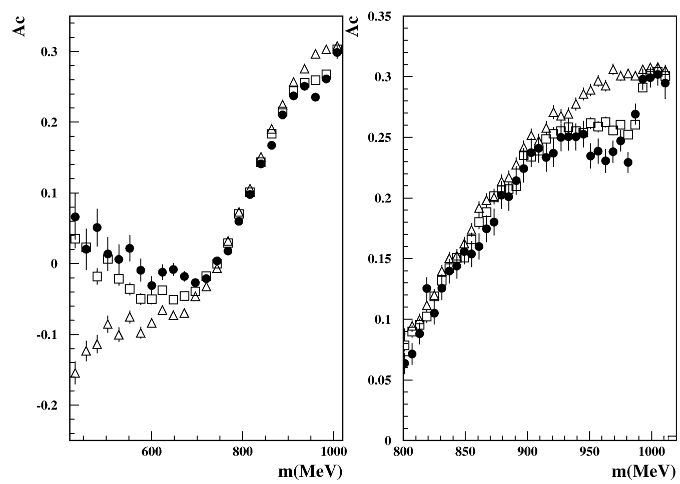

Fig. 6. The forward–backward asymmetry data (full circles) compared to the Monte Carlo expectations based on the non-scalar part of the spectrum only (open triangles), and on the non-scalar plus f_0 part obtained from the KL amplitude (open squares). The right plot shows the detail of the comparison in the f_0 region.

can be understood since in this case the fit prefers a constructive interference term, hence the scalar term has a smaller size.

Using the results of the KL fit, we predict the dependence of the cross-section $\sigma(e^+e^- \to \pi^+\pi^-\gamma, 45° < \theta_\gamma < 135°, 900 < m < 1000\ \mathrm{MeV})$ on $\sqrt{s}$. The predicted behaviour is compared to the data in Fig. 5, in the $\sqrt{s}$ range between 1016 and 1023 MeV. Besides the "on-peak" data sliced in 0.1 MeV wide bins, we show two "off-peak" points taken at $\sqrt{s} = 1017$ and 1022 MeV, respectively. We observe a good agreement for the on-peak data, and a marginal agreement for the two off-peak points.

Finally, following the suggestion contained in Ref. [27], we compared the behaviour of the forward–backward asymmetry as a function of m, shown in Fig. 1(b), with a simulation including the f_0 contribution besides the ISR and FSR [28], and the effect of the $\pi^+\pi^-\pi^0$ background that dilutes the asymmetry in the low mass region. The comparison is shown in

Fig. 6. The KL parametrisation of the f_0 amplitude has been used. The inclusion of the $f_0\gamma$ term is essential to have an acceptable agreement between data and simulation in the region of the f_0 peak and also in the low mass region. This means that the low mass tail of the $f_0\gamma$ amplitude that is cancelled in the m spectrum by the destructive interference with FSR, is on the contrary well evident in the A_c spectrum due to the interference with ISR.

6. Conclusion

Summarising, we found a clear evidence for the process $\phi \to f_0(980)\gamma \to \pi^+\pi^-\gamma$ in the $\pi\pi$ invariant mass spectrum and in the behaviour of the forward–backward asymmetry. An acceptable description of the data is obtained with fits KL and NS. Both fits predict the f_0 to be strongly coupled to kaons, the ratio R between $g^2_{f_0K^+K^-}$ and $g^2_{f_0\pi^+\pi^-}$ being well above 2 as in the KLOE measurement of $f_0 \to \pi^0\pi^0$ [3]. The coupling to the ϕ, $g_{\phi f_0\gamma}$ is found using the NS approach and is in the range 1.2–2 GeV^{-1}. A marginal agreement is obtained by applying the fit SA.

Acknowledgement

We warmly acknowledge N.N. Achasov for many clarifications concerning the KL model; G. Isidori, L. Maiani and S. Pacetti for the development of the NS model here discussed and for many useful discussions; M.E. Boglione and M.R. Pennington for providing us the scattering amplitudes used in the fit and O. Shekhovtsova for the asymmetry simulation.

We thank the DAΦNE team for their efforts in maintaining low background running conditions and their collaboration during all data-taking. We want to thank our technical staff: G.F. Fortugno for his dedicated work to ensure an efficient operation of the KLOE Computing Center; M. Anelli for his continuous support to the gas system and the safety of the detector; A. Balla, M. Gatta, G. Corradi and G. Papalino for the maintenance of the electronics; M. Santoni, G. Paoluzzi and R. Rosellini for the general support to the detector; C. Piscitelli for his help during major maintenance periods. This work was supported in part by DOE grant DE-FG-02-97ER41027; by EURODAPHNE, contract FMRX-CT98-0169; by the German Federal Ministry of Education and Research (BMBF) contract 06-KA-957; by Graduiertenkolleg 'H.E. Phys. and Part. Astrophys.' of Deutsche Forschungsgemeinschaft, Contract No. GK 742; by INTAS, contracts 96-624, 99-37; and by the EU Integrated Infrastructure Initiative HadronPhysics Project under contract number RII3-CT-2004-506078.

References

[1] N.N. Achasov, V.N. Ivanchenko, Nucl. Phys. B 315 (1989) 465.
[2] F.E. Close, N. Isgur, S. Kumano, Nucl. Phys. B 389 (1993) 513.
[3] A. Aloisio, et al., KLOE Collaboration, Phys. Lett. B 537 (2002) 21.
[4] A. Aloisio, et al., KLOE Collaboration, Phys. Lett. B 536 (2002) 209.
[5] R.R. Akhmetshin, et al., CMD-2 Collaboration, Phys. Lett. B 462 (1999) 371.
[6] A. Aloisio, et al., KLOE Collaboration, Phys. Lett. B 606 (2005) 12.
[7] M. Adinolfi, et al., Nucl. Instrum. Methods A 488 (2002) 1.
[8] M. Adinolfi, et al., Nucl. Instrum. Methods A 482 (2002) 364.
[9] M. Adinolfi, et al., Nucl. Instrum. Methods A 492 (2002) 134.
[10] C. Bini, S. Ventura, Search for $f_0(980) \to \pi^+\pi^-$ in $\pi^+\pi^-\gamma$ events with a photon at large angle, KLOE Note 206, October 2005, http://www.lnf.infn.it/kloe/pub/knote/kn206.ps.
[11] F. Binner, J. Kühn, K. Melnikov, Phys. Lett. B 459 (1999) 279.
[12] N.N. Achasov, V.V. Gubin, Phys. Rev. D 57 (1998) 1987.
[13] N.N. Achasov, V.V. Gubin, Phys. Rev. D 56 (1997) 4084.
[14] J.H. Kühn, A. Santamaria, Z. Phys. C 48 (1990) 445.
[15] S. Eidelman, et al., Particle Data Group, Phys. Lett. B 592 (2004) 1.
[16] G. Isidori, L. Maiani, S. Pacetti, private communication.
[17] S.M. Flatté, Phys. Lett. B 63 (1976) 224.
[18] D. Barberis, et al., Phys. Lett. B 462 (1999) 462.
[19] E.M. Aitala, et al., Phys. Rev. Lett. 86 (2001) 765.
[20] G. Colangelo, AIP Conf. Proc. 756 (2005) 60, hep-ph/0501107.
[21] M. Boglione, M.R. Pennington, Eur. Phys. J. C 30 (2003) 503.
[22] T_{11} and T_{12} are improved versions of the amplitudes described in [21], M.R. Pennington, private communication.
[23] C. Bini, Study of scalar meson decays in $\pi^+\pi^-\gamma$ events, KLOE Note 207, October 2005, http://www.lnf.infn.it/kloe/pub/knote/kn207.ps.
[24] E.M. Aitala, et al., Phys. Rev. Lett. 86 (2001) 770.
[25] M. Ablikim, et al., Phys. Lett. B 598 (2004) 149.
[26] A. Denig, F. Nguyen, The KLOE luminosity measurement, KLOE Note 202, July 2005, http://www.lnf.infn.it/kloe/pub/knote/kn202.ps.
[27] H. Czyż, A. Grzelinska, J.H. Kühn, Phys. Lett. B 611 (2005) 116.
[28] G. Pancheri, O. Shekhovtsova, G. Venanzoni, hep-ph/0506332.